European Journal of Pharmaceutical Sciences 172 (2022) 106153

Contents lists available at ScienceDirect

European Journal of Pharmaceutical Sciences

journal homepage: www.elsevier.com/locate/ejps

Quercetin, Rutin And Quercetin-Rutin Incorporated Hydroxypropyl β-Cyclodextrin Inclusion Complexes

Ebru BAŞARAN [1,*], A. Alper ÖZTÜRK [1], Behiye ŞENEL [2], Müzeyyen DEMİREL [1], Şenay SARICA [3]

[1] Anadolu University, Faculty of Pharmacy, Department of Pharmaceutical Technology, Eskisehir, Turkey
[2] Anadolu University, Faculty of Pharmacy, Department of Pharmaceutical Biotechnology, Eskisehir, Turkey
[3] Gaziosmanpasa University, Faculty of Agriculture, Department of Animal Science, Tokat, Turkey

ARTICLE INFO

Key words:
Quercetin
Rutin
Inclusion complex
Freeze drying
Solvent evaporation
DPPH

ABSTRACT

Quercetin (Q) and rutin (R) are well known and most studied flavonoids due to their activities in reduction of inflammation, oxidative damage, platelet aggregation and inhibition of cancer proliferation. Despite their remarkable potentials they have limited oral bioavailability due to the low water solubility. Therefore in this study inclusion complexes of Q and R with hydroxypropyl-β-cyclodextrin (HP-β-CD) were formulated to improve the aqueous solubility, antiproliferative efficacy and also antioxidant activity of the flavonoids. According to the analyses results, aqueous solubilities of Q and R were increased up to ~630 fold and ~55 fold, respectively. ZP values were ranged between -21.7±0.3 mV and -6.1±0.8 mV showing the anionic structure of the complexes. ^{1}H-NMR analyses revealed the complex formation considering the shifts of the protons of the APIs as well as HP-β-CD. The *in vitro* release analyses revealed that the cumulative release of Q was decreased from 22.9 % to 18.1 and 15.2 for T9 and T 24 formulations respectively while the cumulative release of R increased from 26.8 % up to 64.5 % and 75.8 % with T14 and T24 formulations respectively. According MTT analyses results, Q showed higher antiproliferative effect in MDA-MB-231 and A549 cell lines compared to NIH-3T3 cell lines while R showed remarkable effect only on MDA-MB-231 cell lines at the end of 48 h of incubation period. A synergistic effect was observed in the formulation of combined flavonoid (Q/R) inclusion complexes and an antiproliferative effect was ordered as MDA-MB-231 > A549 > NIH-3T3. The selected complexes T9 (Q), T14 (R) and T24 (Q/R) have shown the highest antioxidant activity with 93.8 %, 65.3 % and 93.1 % respectively with DPPH analyses. In conclusion incoporation of Q, R and Q/R to HP-β-CD based inclusion complexes have great potentials with enhanced *in vitro* dissolution characteristics and antiproliferative effects on different types of cancer cell lines for efficient treatment of severe disorders.

1. Introduction

Flavonoids are plant originated polyphenolic compounds which play very important role in free radical trapping by acting as chelators (Iacopini et al.,2008; Alsaif et al.,2020). In many cases free radicals were regarded as the leading reasons of many diseases like aging, tissue damage, Parkinson's disease, Alzheimer's disease, neuroprotective effect in epilepsy, diabetes mellitus, cardiovascular diseases. They have also protection ability against oxidative stress and UV damages, and also show enzymatic activity and gene expression modulations, as well as viral, fungal, and bacterial protections (Wang et al.,2021; Akyuz et al., 2021; Ilyich et al.,2021). Inhibitory effects on cancer cell lines were also reported (Paodel et al, 2021; Tripathi et al, 2021). Among the polyphenolic group members, Quercetin (3,3′,4′,5,7-pentahydroxyflavone) (Q) is one of the most studied flavonoid due to its activities in reduction of inflammation, oxidative damage, platelet aggregation, and capillary permeability. Q also exhibits antiviral, antiinflammatory, anticancer, antiobesity activities with protective activities in cardiovascular, hepatoprotective, and neuroprotective activities with antidepressant activity however its pharmaceutical potential was limited due to the low water solubility related limited oral bioavailability (D'Andrea 2015; Güleç and Demirel 2016; Zhang, Ning, and Wang 2020). Rutin (R) (quercetin-3-O-rutinoside or 3′,4′,5,7-tetrahy- droxy-flavone-3-rutin oside) is also a well known flavonoid with anti-inflammatory,

* Corresponding author: Mrs. EBRU BAŞARAN, Pharmaceutical Technology, Anadolu University: Anadolu Universitesi, Anadolu University Faculty of Pharmacy, 26470 Eskisehir, Turkey. Tel : +90 533 7127422.
E-mail address: ebcengiz@anadolu.edu.tr (E. BAŞARAN).

https://doi.org/10.1016/j.ejps.2022.106153
Received 15 October 2021; Received in revised form 19 February 2022; Accepted 23 February 2022
Available online 26 February 2022

Table 1
Compositions and preparation methods of the complexes.

Code	Method	Shaking time (h)	Q (mg)	R (mg)	HP-β-CD (mg)	Ethanol (mL)	Water (mL)
T9	FD	24	10.00	-	48.30	32	32
T10	FD	-	10.00	-	48.30	32	32
T11	SE	24	10.00	-	48.30	32	32
T12	SE	-	10.00	-	48.30	32	32
T13	FD	24	-	10.00	23.94	32	32
T14	FD	-	-	10.00	23.94	32	32
T15	SE	24	-	10.00	23.94	32	32
T16	SE	-	-	10.00	23.94	32	32
T21	FD	24	9.40	9.40	30.00	32	32
T22	FD	-	9.40	9.40	30.00	32	32
T23	SE	24	9.40	9.40	30.00	32	32
T24	SE	-	9.40	9.40	30.00	32	32

*FD: Freeze drying; SE: Solvent evaporation.

antiplatelet, vasoactive, antihypertensive, antiallergic, antispasmodic, hypolipidaemic, cytoprotective, antitumor, antiprotozoal, antibacterial, and antiviral activities even for possible Inhibition of SARS-CoV-2 vital proteins. R also has low water solubility which limits its therapeutic use (Ekaette and Saldaña 2021; Paudel et al., 2021; Rahman et al.,2021).

Cyclodextrins (CDs) are natural cyclic oligosaccharides containing six, seven and eight glucopyranose units (named α-CD, β-CD and γ-CD respectively) obtained from the enzymatic degradation of starch. They have truncated conical structure having a hydrophobic interior and hydrophilic outer structure containing primary and secondary -OH groups (Chen et al.,2017). In an aqueous environment, these carbohydrates (host molecule) can locate the lipophilic agents (guest molecule) in their inner cavities forming highly water soluble inclusion complexes with the help of water soluble outer surfaces while enhancing the stability of incorporated agent (Hammoud et al.,2020; Buko et al.,2020; Liu et al.,2021). Besides natural CDs many functional groups can also be incorporated into the structures which enhances the water solubility in great extend with different inner cavity dimentions (Challa et al.,2005).

Among the commonly used CDs, hydroxypropyl-β-cyclodextrin (HP-β-CD) is one of the most used CD due to high water solubility (> 600 mg/mL), low cost, low toxicity and high solubility enhancement ability makes HP-β-CD preferential even for parenteral applications. HP-β-CD has a hydrophobic cavity of size range of 0.60 - 0.65 nm which gives possibility to incorporate large scale of active agents (Al-Qubaisi et al., 2019; Wang et al.,2020; Melo et al.,2020).

A literature search revealed several papers dealing with the use of various types of CDs for the enhancement of water solubility of Q (Zheng and Chow 2009; Kellici et al. 2016; Manta et al. 2020; Park et al. 2017) and R (Paczkowska et al. 2015; Savic et al. 2016; Franco and De Marco 2021) using different preparation methods. For example, Celik et al. (2015) have studied Q and R inclusion complexes with β-CD and HP-β-CD in solution while Sri et al (2007) have prepared inclusion complexes in solid state by kneading and co-evaporation method. However, none of the former studies have tried to incorporate both Q and R at the same time into the inclusion complexes. Taking into consideration the former studies, in this study Q, R and Q/R were incorporated into HP-β-CD inclusion complexes with freeze drying and solvent evaporation methods. Characterization studies were performed in detail. The possible synergistic effect of combined flavonoids on antioxydant activity as well as the toxicity were also evaluated.

2. Materials and Methods

2.1. Materials

Quercetin, Rutin hydroxypropyl β-cyclodextrin, ethanol, methanol, acetic acid, hydrochloric acid and potassium chloride were purchased from Sigma-Aldrich (Steinheim, Germany). 2,2-diphenyl-1-picrylhydrazyl (DPPH) was purchased from Fluka (Steinheim, Germany). Deutero chloroform was from Merck (Darmstadt, Germany). Spectrophotometry-grade dimethyl sulfoxide (DMSO), Dulbecco's Modified Eagle's Medium (DMEM), tyripsin/EDTA solution (0.25 %), and MTT dye were purchased from Sigma-Aldrich (Darmstadt, Germany). Fetal bovine serum, penicillin, and streptomycin solution were purchased from Capricorn Scientific GmbH (Ebsdorfergrund, Germany). All other chemicals were of analytical grade.

2.2. Determination of Q and R by HPLC

For the determination of the active agents, modified HPLC method was used (Zhao et al. 2011). Shimadzu LC-20 AT, (Japan), Inertsil ODS-3 C18 column (150 mm x 4.6 mm, 5 μm) (GL Sciences, Japan) with auto injector (Shimadzu, Japan) was used. Methanol : water : acetic acid (5 %) 65 : 33 : 2 (v / v / v) was determined as the mobile phase (1 mL. min^{-1}). Analyses were performed at 373 nm with 40 °C column temperature. According to ICH guidelines validation studies were performed (ICH 1995).

2.3. Determination of complex formation equilibration time

Complex formation equilibrium time was determined by comparing the solubility data in HP-β-CD solution. Briefly; HP-β-CD stock solution (10 mM) was prepared and excess amount of Q and R and Q/R (1:1, w/w) were added to HP-β-CD solution and strongly agitated (300 rpm) using a horizontal shaker (WiseShake SHR-1D, Korea) up to 72 hours. At predetermined time intervals samples were taken and filtered through the pre-saturated polyamide membrane filter (0.22 μm) and were analyzed by HPLC. The time where solubility of the active agents remained unchanged regarded as the equilibrium time for the complexes (Loftsson et al., 2005; Al-Heibshy et al., 2020).

2.4. Preparation of inclusion complexes

Freeze drying (Laquintana et al.,2019; Qu et al.,2021) and solvent evaporation methods (H Wang et al. 2020.) were used for the preparation of the complexes. In freeze dring method HP-β-CD was dissolved in ultra pure water while Q and R were dissolved in ethanol. Mixtures were vigorously shaken after the addition of flavonoid solution onto the CD solution at 300 rpm during the equilibrium period with being protected from direct sunlight. At the end of the shaking period the ethanol was evaporated under constant stirring at room temperature (25°C ±2°C) for 12 hours and mixtures were frozen at -80°C (New Brunswick Sci., USA) and freeze dried (Leybold-Heraeus Lyovac GT-2, Germany) (Laquintana et al.,2019; Qu et al.,2021).

In solvent evaporation method HP-β-CD was dissolved in ultra pure water while Q and R were dissolved in ethanol. The mixtures were vigorously shaken at 300 rpm during the equilibrium period with protection from direct sunlight. At the end of the shaking period the mixtures were dried using Büchi R-205 (Switzerland) rotary evaporator at

Table 2
Results of yield %, entrapment efficiency %, aqueous solubility and zeta potential analyses results of the complexes (mean ± SE).

Code	Method*	Shaking Time (h)	Active Agent	Yield %	EE %	Aqueous Solubility (μg/mL)**	ZP (mV)
-	-	-	Q	-	-	1.5 ± 0.0	-
-	-	-	R	-	-	34.3 ± 0.1	-
T9	FD	24	Q	63.5 ± 10.7	95.5 ± 0.7	548.3 ± 0.0	-13.0 ± 0.1
T10	FD	-	Q	59.9 ± 25.4	88.9 ± 0.7	945.6 ± 0.0	-11.6 ± 0.1
T11	SE	24	Q	67.0 ± 1.83	92.6 ± 1.98	547.9± 0.0	-20.6 ± 0.3
T12	SE	-	Q	48.0 ± 10.8	88.64 ± 5.6	174.2 ± 0.0	-21.7 ± 0.3
T13	FD	24	R	73.2 ± 9.3	95.4 ± 4.3	488.3 ± 0.1	-6.1 ± 0.8
T14	FD	-	R	56.8 ± 21.5	94.9 ± 1.4	1901.4 ± 0.0	-6.5 ± 0.4
T15	SE	24	R	46.8 ± 13.2	88.5 ± 6.2	929.5 ± 0.0	-12.9 ± 1.1
T16	SE	-	R	68.3 ± 10.7	92.7 ± 6.1	668.6 ± 0.0	-14.3 ± 0.4
T21	FD	24	Q	45.2 ± 14.7	81.0 ± 5.7	89.8 ± 0.0	-16.3 ± 0.3
			R		86.2 ± 5.6	705.0 ± 0.0	
T22	FD	-	Q	76.3 ± 7.3	90.3 ± 0.5	71.7 ± 0.0	-20.4 ± 0.2
			R		97.1 ± 1.3	525.9 ± 0.0	
T23	SE	24	Q	49.9 ± 6.8	100.6 ± 2.4	141.6± 0.0	-11.2 ± 0.5
			R		81.9 ± 2.3	904.7 ± 0.0	
T24	SE	-	Q	52.6 ± 11.0	91.0 ± 1.7	136.5 ± 0.1	-11.0 ± 1.2
			R		100.0 ± 1.7	1271.0 ± 0.0	

*FD: Freeze drying; SE: Solvent evaporation.
** determined as the amount dissolved in water after 1 h under vigorous agitation.

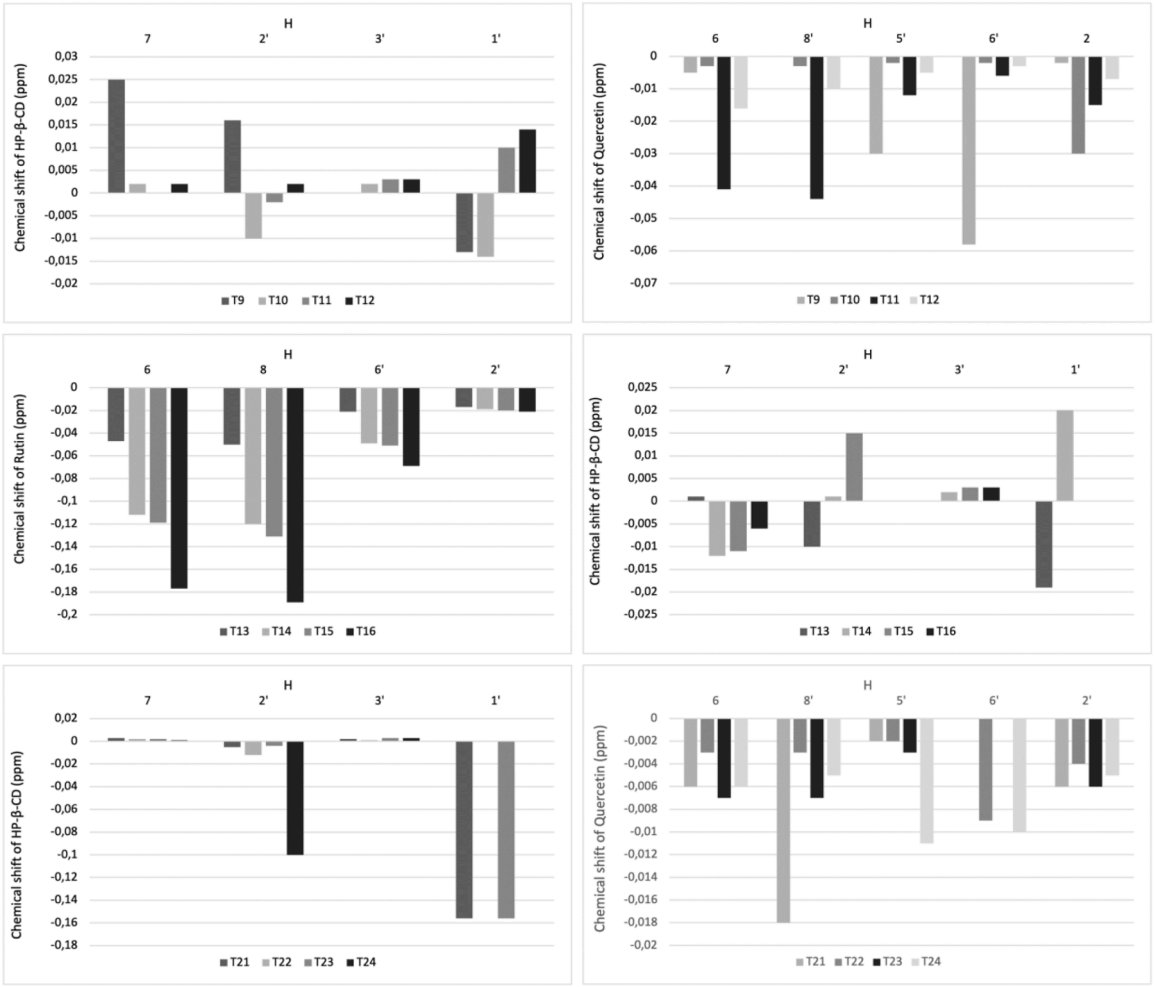

Fig. 1. Chemical shifts of the complexes.

50 °C ± 1°C under 100 mbar (Wang et al.,2020). For the determination of shaking effect on the complex formations same formulations were prepared without shaking step. The compositions of the prepared formulations were presented in Table 1.

2.5. Determination of the entrapment efficiency

For the determination of entrapment efficiency (EE) % of the complexes, accurately weighed formulations were dissolved in mobile phase and Q and R amounts were determined by validated HPLC analyses. EE

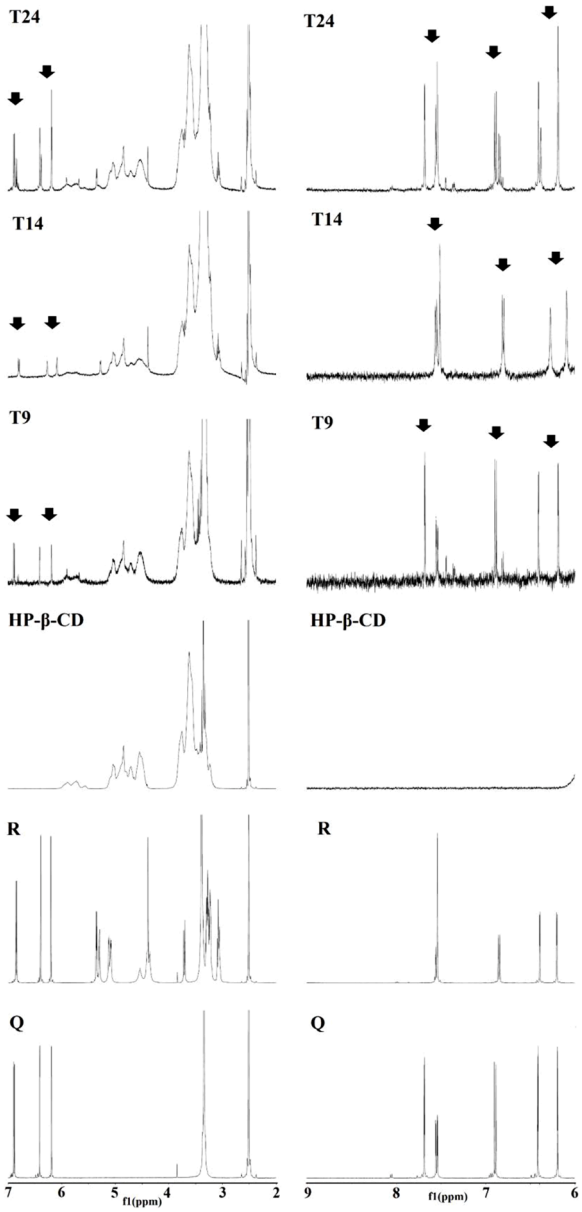

Fig. 2. ^{1}H-NMR spectra of Q, R, HP-β-CD, and the selected complexes.

% of the complexes were calculated by using the **Equation 1** (Nicoletti et al. 2020).

$$\text{EE}\ (\%) = [\text{Determined drug quantity}\ (\text{mg})]/[\text{Theoretical drug quantity}\ (\text{mg})] \times 100 \quad (1)$$

2.6. Physicochemical characterization

2.6.1. Zeta potential analyses

Zeta potential (ZP) analyses were performed using Zetasizer Nano ZS (Malvern, UK) at 25 °C ± 2 °C in distilled water.

2.6.2. Nuclear magnetic resonance spectroscopy analyses

Proton nuclear magnetic resonance (^{1}H-NMR) analyses were performed using Bruker 500 MHz UltraShield NMR (Germany) on pure Q, pure R, pure HP-β-CD, physical mixtures (PMix) and the inclusion complexes. Deutero chloroform ($CDCl_3$) was used as a solvent for the analyses. Chemical shifts were given in ppm relative to tetramethylsilane as an internal standard (δ=0).

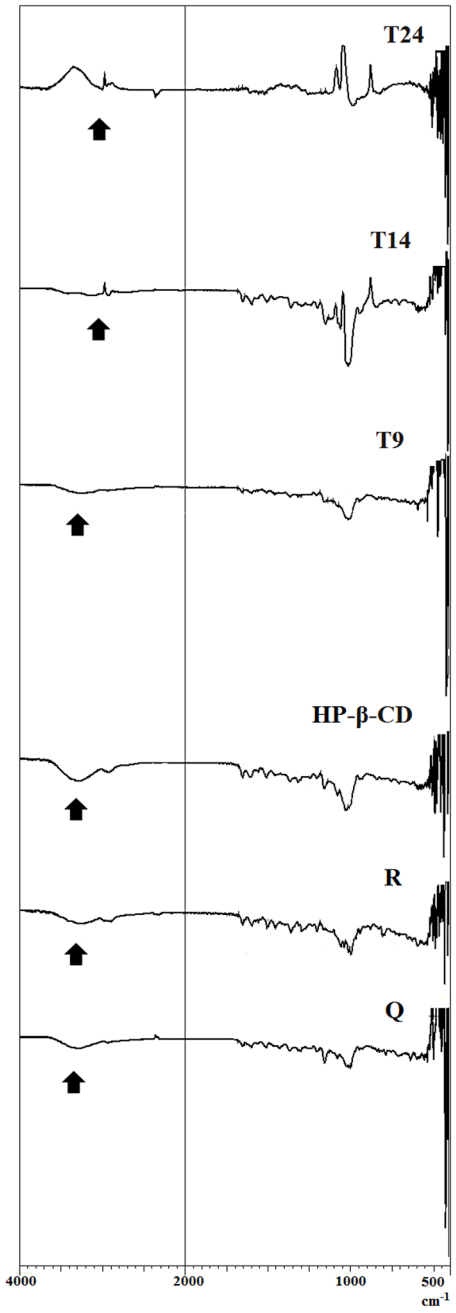

Fig. 3. FT-IR spectra of Q, R, HP-β-CD, and the selected complexes.

2.6.3. Fourier transform infrared spectrophotometry analyses

Fourier-transform infrared spectroscopy (FT-IR) spectra of powdered samples (pure Q, pure R, pure HP-β-CD, PMix and the inclusion complexes) were recorded by Shimadzu IR Prestige-21 (Japan) within 4000-500 cm^{-1} with 1 cm^{-1} resolution.

2.6.4. Thermal analyses

Differential scanning calorimetry (DSC; Shimadzu DSC-60, Japan) analyses were used for determination of thermal behaviours of pure Q, pure R, pure HP-β-CD, PMix and the inclusion complexes. The samples (4 - 5 mg) were sealed into aluminium pans and were heated from 30 °C to 350 °C with 10 °C.min^{-1} increase rate under nitrogen atmosphere (50 mL. min^{-1}). An empty aluminum pan was used as a reference during the analyses.

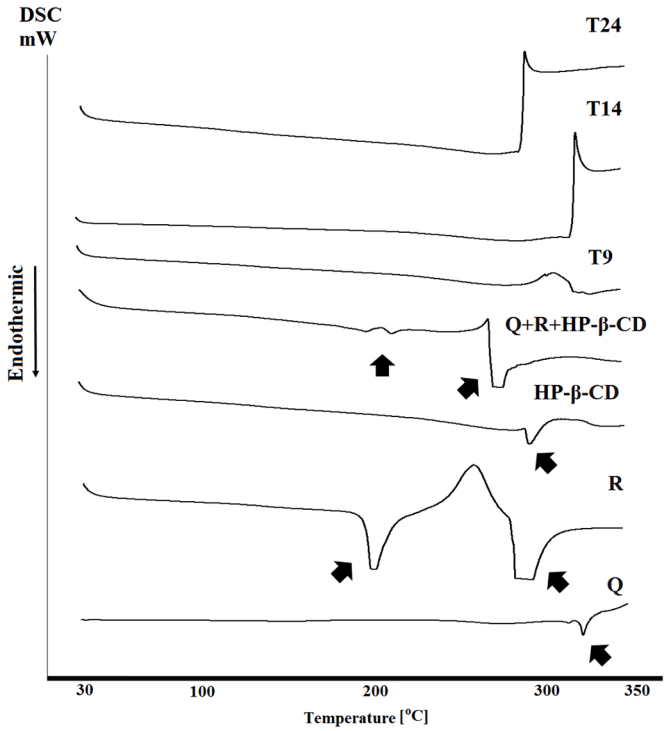

Fig. 4. Thermograms of Q, R, HP-β-CD, physical mixture (Q + R + HP-β-CD) and the selected complexes.

2.6.5. *X-Ray difraction analyses*

X-ray powder diffractometry (XRD) analyses of powdered samples (pure Q, pure R, pure HP-β-CD, PMix and the inclusion complexes) were performed with D/MAX Rint 2000 diffractometer (Rigaku, Japan) using CuKα as a radiation source (λ= 1.5418 Å, 40 KV and 30 mA) generated at 40 kVand 30 mA current intensity with a scan rate at 2Θ and 2° min^{-1} in the range of 2° - 40° angles.

2.6.6. *In vitro dissolution and release kinetics*

Prior to the *in vitro* dissolution studies, the amount of Q, R and inclusion complexes that can be dissolved in water after 1 h under vigorous agitation, was evaluated. Excess amounts of API's and formulations were added to 2 mL of distilled water and the Q and R concentration reached after 1 h under vigorous stirring in water at 25 °C ± 2 °C, was evaluated prior to *in vitro* release studies. At the end of the shaking period dispersions were filtered through 0.45 μm polyamide membrane filter and were analyzed by HPLC (Al-Heibshy et al.,2020). *In vitro* dissolution studies of Q and R from HP-β-CD complexes were investigated with dialysis membrane method (Shen and Burgess 2013; Zhou et al.,2020). To simulate gastric fluid, a dissolution medium of pH 1.2 should be employed without enzymes (FDA 1997). In our study complexes containing 1 mg Q and/or 1 mg R was placed in a dialysis bag (Membra-Cel® MC18 × 100 CLR, Viskase Companies, USA) with MWCO 14000 Da. 1 mL of dissolution medium was added inside the membrane and the bag was sealed from both ends and placed into an amber glass beaker containing 50 mL 0.1N HCl (pH 1.2) solution at 37 °C ± 0.5 °C as the dissolution medium under 100 rpm (WiseStir, Daihan, Korea) stirring. For the prevention of evaporation as well as the protection of Q and R from direct light the receptor compartment was fully covered during the analyses. At determined time intervals the samples (1 mL) were collected and the volume of dissolution medium was kept constant with addition of fresh medium to maintain sink conditions. The withdrawn samples were filtered through pre-saturated polyamide membrane filter (0.22 μm) and were analyzed by HPLC. The experiments were carried out in triplicate. DDSolver software program was used for the evaluation of release kinetics of the complexes (Zhang et al.,2010).

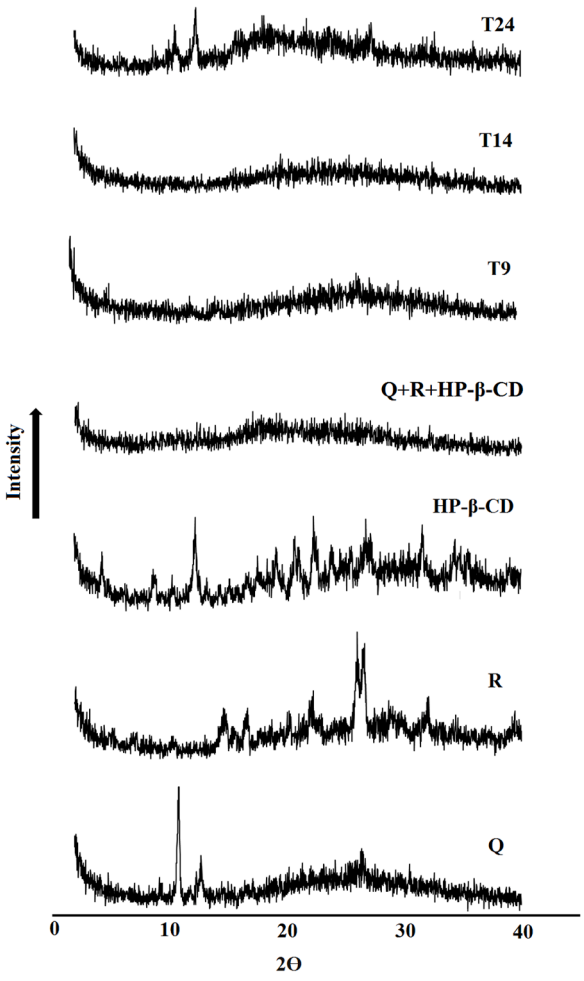

Fig. 5. XRD diffractograms of Q, R, HP-β-CD, physical mixture (Q+R+HP-β-CD) and the selected complexes.

2.7. *Cytotoxicity study*

The MTT test, developed by Mosmann (1983), is a simple experiment based on the conversion of MTT into formazan crystals by living cells with mitochondrial function and therefore MTT tests were used to determine the activity of prepared compounds and pure substances on different cell lines in our study (Kamiloglu et al., 2020). Three different types of cell were used for the determination of cytotoxicity as well as anticancer activity of the formulations prepared. 3T3 mouse fibrolast cell lines were used as non-cancerous cell line for the evaluation of cytotoxicity of the complexes (Danihelová 2013). Anticancer activity of the prepared formulations were evaluated on two different types of cancer cell lines; Human Breast Adenocarcinoma (MDA-MB-231) and Human Lung Carcinoma cell lines (A549) (Li et al., 2021; Komi et al., 2022). Briefly, 2 × 10^4 cells were seeded into 96-well plates on the first day and allowed to incubate. The next day, various concentrations of test compounds in fresh cell culture medium were applied to the wells and left to incubate for 48 hours. After 48 hours of incubation, the components from the wells were withdrawn and 20 μL of MTT dye (5 mg/mL in PBS) was added to the wells. It was left to an extra incubation for 3 hours and 200 μL of DMSO was added to dissolve the formazan crystals onto the wells by drawing the dye. After incubating for half an hour, the color change was read as absorbance at 570 nm in a multi-plate reader (Cytation 5, BioTek, England). The intensity of the colored product in these results is directly proportional to the number of viable cells in the culture. Only wells with added cell culture medium to which no specimens were applied were used as controls their absorbance was

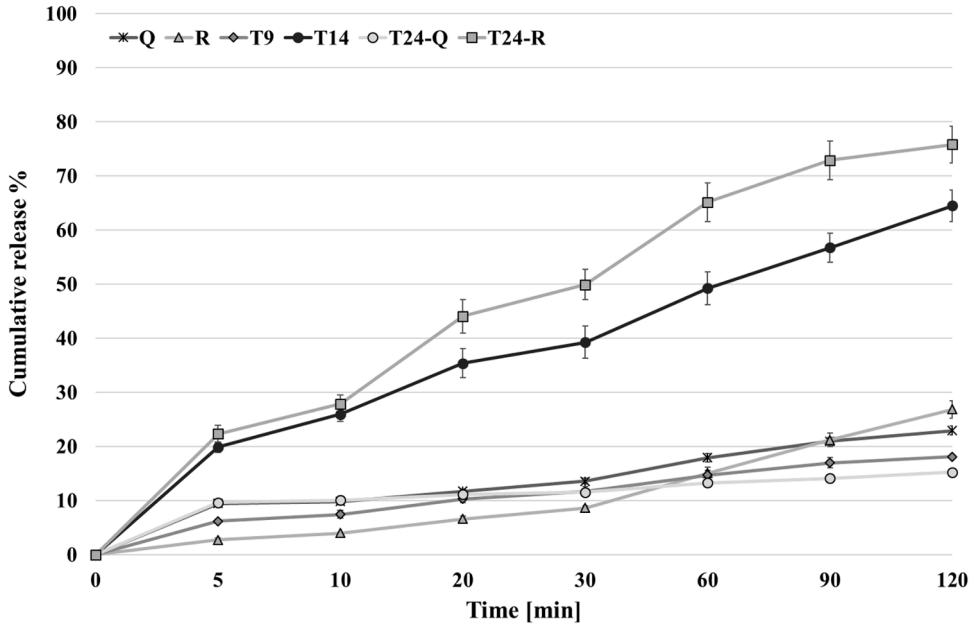

Fig. 6. Dissolution profiles of T9, T14, T24 and pure Q and R (n = 3; mean ± SE).

Table 3
Release kinetic modeling of complexes.

Kinetic Model		Formulation Codes					
		Pure Q	**Pure R**	**T9**	**T14**	**T24 Q**	**T24 R**
Zero Order	**k_0 (mg × min^{-1})**	0.000 ± 0.000	0.000 ± 0.000	0.000 ± 0.000	0.001 ± 0.000	0.000 ± 0.001	0.001 ± 0.000
	r^2	0.001	0.001	0.000	0.000	-0.010	0.000
	AIC	0.031	0.036	0.038	0.055	0.042	0.058
First order	**k_1 (min^{-1})**	0.000 ± 0.000	0.000 ± 0.001	0.000 ± 0.002	0.000 ± 0.000	0.000 ± 0.000	0.000 ± 0.000
	r^2	0.001	0.001	0.000	0.000	-0.009	0.001
	AIC	0.030	0.033	0.037	0.051	0.041	0.049
Higuchi	**k_H (mg × $min^{-1/2}$)**	0.002 ± 0.001	0.003 ± 0.000	0.002 ± 0.000	0.006 ± 0.000	0.002 ± 0.000	0.008 ± 0.000
	r^2	**0.001**	**0.001**	0.001	0.001	-0.002	0.001
	AIC	**0.004**	**0.023**	0.022	0.038	0.033	0.042
Korsmeyer-Peppas	**$k_{K\text{-}P}$ (min^{-n})**	0.005 ± 0.000	0.001 ± 0.000	**0.004** ± 0.000	**0.012** ± 0.000	**0.007** ± 0.000	**0.012** ± 0.000
	n*	0.000 ± 0.000	0.001 ± 0.000	0.000 ± 0.000	0.000 ± 0.000	0.000 ± 0.000	0.000 ± 0.000
	r^2	0.001	0.001	**0.001**	**0.001**	**0.001**	**0.001**
	AIC	0.009	0.025	**0.000**	**0.016**	**0.002**	**0.035**
Hixson-Crowell	**$k_{H\text{-}C}$ ($mg^{1/3}$ × min^{-1})**	0.000 ± 0.000	0.000 ± 0.001	0.000 ± 0.000	0.000 ± 0.000	0.000 ± 0.010	0.000 ± 0.000
	r^2	0.001	0.001	0.000	0.000	-0.009	0.001
	AIC	0.030	0.034	0.037	0.052	0.041	0.052

*n is the parameter indicative of the drug release mechanism for the Korsmeyer-Peppas Model.

Table 4
IC_{50} values of Q, R, HP-β-CD and the selected complexes.

	IC50 (μM)					
	Q	**R**	**HP-β-CD**	**T9**	**T14**	**T24**
NIH-3T3	80.49	>200	>200	32.3	>200	175
MDA-MB-231	52	155	>200	>200	192.5	105.8
A549	74	>200	>200	>200	>200	141.7

accepted as 100 % cell viability. The data obtained from the other wells were proportional to the control wells and reflected in the graph as % value (Sahinturk et al. 2018).

2.8. Antioxidant activity with DPPH

Antioxidant activity of the pure Q, R and the HP-β-CD inclusion complexes were tested by determination of free radical scavenging activities using 2,2-diphenyl-1-picrylhydrazyl (DPPH) with minor modifications (Rebolledo et al. 2021). In this method pure flavonoids and their complexes (containing 100 μg Q or R or Q/R) were dissolved in ethanol (5 mL). Ethanolic solutions of Q, R and complexes with different concentrations (5 $\mu g.mL^{-1}$, 15$\mu g.mL^{-1}$, 20 $\mu g.mL^{-1}$) were treated with 2 mL of ethanolic DPPH solution (0.2 mM) and total volumes were adjusted to 4 mL with ethanol. The mixtures were shaken vigorously and kept at room temperature for 30 min as being protected from direct light exposure. The solutions were analyzed at 517 nm with UV-visible spectrophotometer (UV-160A, Shimadzu, Japan) (n = 6) for the determination of decrease in absorbance of the resulting solutions. 2 mL ethanol and 2 mL of ethanolic DPPH solution (0.2 mM) served as positive and negative controls. The DPPH scavenging rates were calculated according to the following **Equation 2** where $A_{control}$ was the absorbance value of the blank and A_{sample} was the absorbance value of tested samples (Wang et al.,2018).

$$\text{DPPH scavenging activity } (\%) = \left[A_{control} - A_{sample} \,/\, A_{control}\right] \times 100 \qquad (2)$$

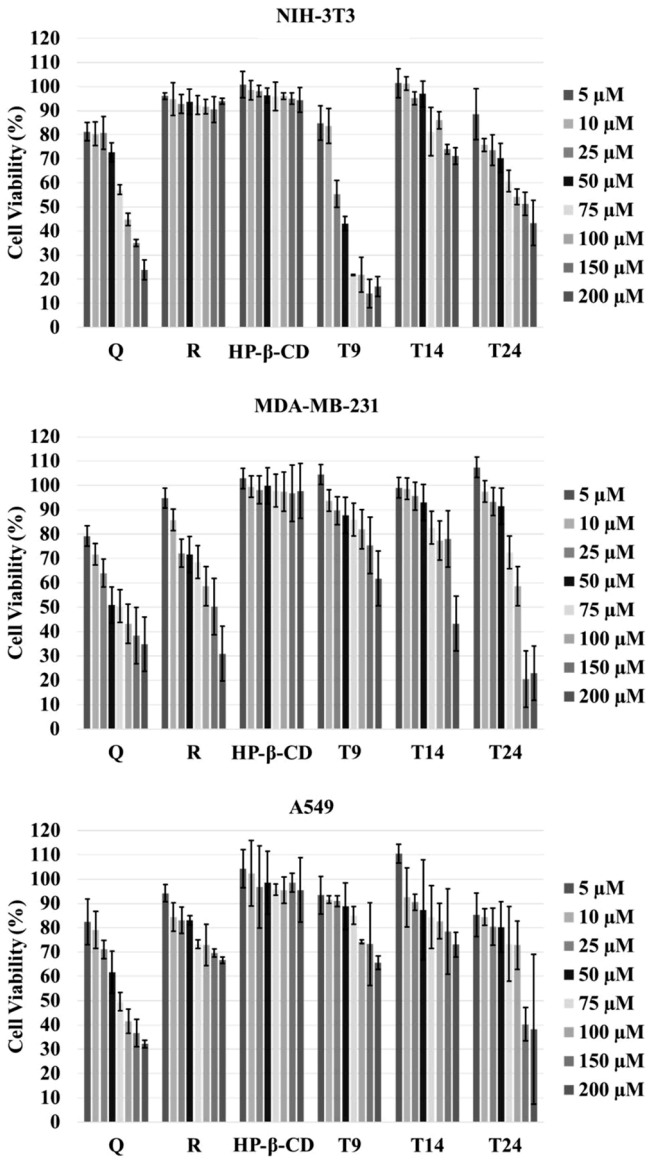

Fig. 7. Cytotoxicity results of Q, R, HP-β-CD and the selected complexes (n = 3; mean ± SD).

2.9. Statistical evaluation

The analyses data were presented as the mean ± standard error (SE). Differences between groups and the control groups were analyzed using regression and one way ANOVA analyses, with Minitab 19. A p-value < 0.05 was considered to be statistically significant.

3. Results and Discussions

3.1. Determination of Q and R by HPLC analyses

In HPLC analyses the linearity range of R and Q was 10-100 µg•mL^{-1} and regression equation was y = 104762x – 40480.42 (slope: 104762.00 ± 5828.89; intercept: -40480.42 ± 43036.39) for Q, and y = 41659.39x – 62273.33 (slope: 41659.39 ± 678.76; intercept: -62273.33 ± 23694.20) for R. Correlation coefficient (r^2) of R was 0.9998 ± 0.0009 and for Q r^2= 0.9996 ± 0.0001. Limit of detection (LOD) and lower limit of quantification (LLOQ) were calculated based on the "Standard Deviation of the Response and the Slope" approach. LOD and LLOQ values for R and Q were found to be 3.253 µg.mL^{-1}, 9.857 µg.mL^{-1} and 2.677 µg.mL^{-1}, 8.112 µg.mL^{-1} respectively. Recovery of the method was 98-102 %. With RSD values of <2 % the method for R and Q was regarded as precise due to repeatability and intermediate precision. Validation studies were performed according to the ICH guidelines and analysis results fulfill the ICH requirements (ICH Q2 R1, 2020).

3.2. Determination of complex formation equilibration time

Formation of CD inclusion complexes alters the physicochemical properties of the guest molecule (Nicoletti et al.,2020). The solubility rates of Q and R and Q/R (1:1, w/w) in HP-β-CD stock solution (10 mM) were evaluated during 72 hours under strong agitation of 300 rpm. At predetermined time intervals samples were taken and were analyzed by HPLC. The solubility of the active agents were remained unchanged after 24 hours therefore equilibrium time for the complexes were stated as 24 hours for further formulation studies.

3.3. Determination of the entrapment efficiency and solubility characteristics

The yields were varied from ~45 % to 76 %. while the amount of the APIs encapsulated into complexes were varied from~ 81 % to 101 % (Table 2). According to the results presented in Table 2, complexation with HP-*β*-CD has remarkably increased the amount of both active agents dissolved in water after 1 h under vigorous agitation. More specifically, an increase from 1.5 µg.mL^{-1} to 945.6 µg.mL^{-1} and from 34.3 µg.mL^{-1} to 1901.4 µg.mL^{-1} was observed for Q and R, respectively, indicating a corresponding increase in the aqueous solubility of both Q and R of about ~630 fold and ~55 fold, respectively, depending on the type of production method (Table 2) (Jantarat et al.,2014).

3.4. Physicochemical characterization

3.4.1. Zeta potential analyses

The ZP values of the colloidal particles are one of the most important paramater for the cellular uptake therefore ZP analyses were performed in this study (Al-Qubaisi et al.,2019). ZP values over ±30 mV regarded as the basic principle of physical stability of the colloidal dispersions considering electrostatic repulsions within the particles (Pinheiro et al., 2020). In our study ZP values of the inclusion complexes were valued -6.1 x to -21.7 mV due to the hydroxyl groups of the HP-β-CD (Table 2) (Yan et al.,2019). Inclusion of R has decreased the ZP values compared to Q incorporated inclusion complexes however when Q and R were incorporated together the ZP values were valued -11 mV to -20 mV (Elmi et al.,2021). And avoidance of shaking step has influenced the ZP values most probably influencing the amount of hydroxyl groups on the surface of HP-β-CD inclusion complexes. Analyses results demonstrated that besides the formulation components, the production method also has an influence on ZP values of the complexes (Table 2) (Remanan and Zhu 2021).

3.4.2. Nuclear magnetic resonance spectroscopy

NMR analysis is most powerful tool used to determine the inclusion of a guest molecule into the hydrophobic CD cavity in solution which can be identified by comparing the chemical shifts of the free guest molecule and CD with those of its complex. Being more sensitive than carbon NMR spectroscopy, proton NMR spectroscopy has been widely used. ^{1}H-NMR analyses were performed for the determination of structural changes with the determination of chemical shifts of the selected protons during complexation process (Laquintana et al.,2019). Formation of the inclusion complexes were clearly determined by ^{1}H-NMR analyses by shifted protons of R, Q and HP-β-CD within the range of 2-7 ppm and 6-9 ppm (Fig. 1).

In ^{1}H-NMR spectrum of HP-β-CD there were several characteristic signals at 5.47–5.92 (m, OH-2, OH-3, 14 H), 5.03 (s, H-C1, 7 H) and 4.84 (s, OH-6, 7 H) ppm and changes in these signals demonstrated the

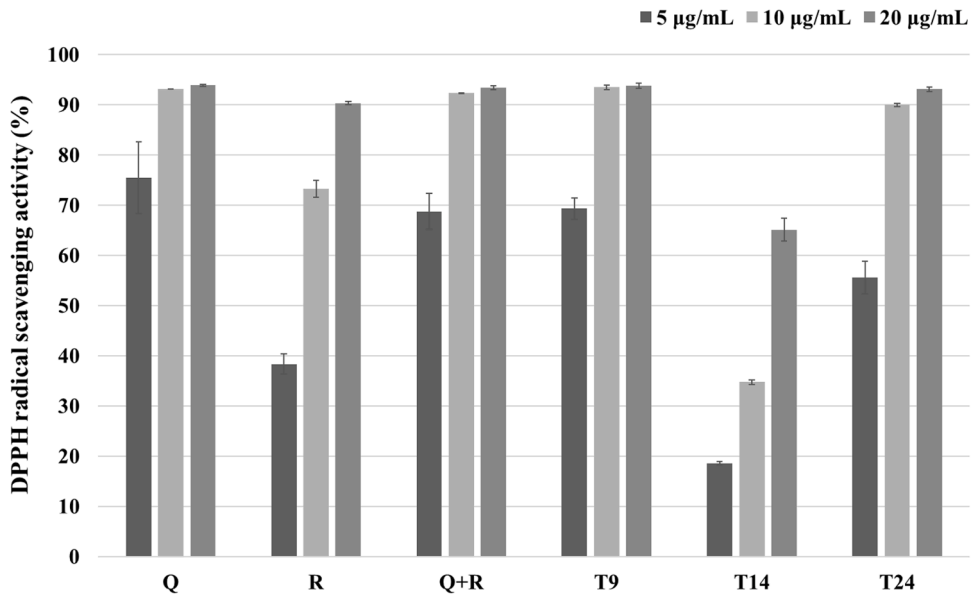

Fig. 8. DPPH analyses results of Q, R, and the selected complexes (n = 3; mean ± SE).

successful binding of Q and R to HP-β-CD (Yan et al.,2019). The presence of Q caused a significant downfield shift for the protons (H2 and H7) of HP-β-CD for T9 formulation. On the other hand, the outside H1 showed a clear up-filed shift, confirming that the H2 and H7 protons were more affected by the guest molecule (Laquintana et al.,2019). The presence of R caused a highest downfield shift of CD's proton 1 (H1) for T14 formulation suggestion that inclusion (Fig. 1). In the ^{1}H-NMR spectra of the formed inclusion compounds, R protons showed an upfield displacement due to a variation of local polarity and, also to the weak interactions with CD cavity hydrogen atoms (Fig. 1) (Nicolescu et al., 2010).

According to the results presented in Table 2 and chemical shift data of ^{1}H-NMR analyses T9, T14, and T24 were selected as optimum complexes for further studies therefore only the results of the analyses of the selected formulations were presented in the manuscript. Spectra illustrated the ^{1}H NMR spectroscopy clearly showed the complex formation in comparison with pure R, Q and HP-β-CD spectra (as ppm) (Fig. 2).

3.4.3. *Fourier transform infrared spectrophotometry*

FT-IR analyses were performed considering the changes in the characteristic signals of pure APIs confirming the formation of the complex as a new compound with different spectroscopic signals (Sri et al.,2007). HP-β-CD showed characteristic peaks of functional groups and vibrations including O-H stretching at 3340 cm^{-1}, H-O-H bending at 1653 cm^{-1}, C-O band of COOH at 1159 cm^{-1}, C-O-C bending at 1028 cm^{-1} (Buko et al.,2020). The Q showed a phenolic -OH band around 3298 cm^{-1}, a characteristic –CO streching at 1653 cm^{-1}, bending and aromatic streching around 1010 cm^{-1}, –OH bending phenolically around 1157 cm^{-1} (Valencia et al., 2021). The signals at 3282 cm^{-1}, 1653 cm^{-1}, 1157 cm^{-1} referring O-H bending, C=O streching and C-O-C respectively detected for pure R (Fig. 3) (Patil and Jobanputra 2015; Remanan and Zhu 2020). Signals of the characteristic bands of Q and R were shifted especially for O-H bending signals showing the formation of inclusion complexes successfully with HP-β-CD (Pereira et al., 2020). For Q; 3298 cm^{-1} signal was shifted to 3277 cm-1 in T9 formulation while for R that band was shifted form 3282 cm^{-1} to 3142 cm^{-1} in T14 formulation. For T24 formulation incorporations of both Q and R have shifted the O-H band to 3001 cm^{-1} (marked with arrows) (Fig. 3).

3.4.4. *Thermal analyses*

DSC analyses gives possiblity to reveal the structural differentiations during complex formations therefore reduction in the intensities, appearance and/or dissapearance of the signals together with a shift to other peaks referes to mostly formation of new interactions and successful formation of complexes (Wang et al., 2020; Valencia et al., 2021). In our study pure Q and R showed endothermic peaks at 315 °C and 198 °C respectively (Fig. 4). The possible melting/decomposition peak was revealed at 298 °C for R which was also revealed in the thermogram of physical mixture. The thermogram of HP-β-CD corresponded to the melting and decomposition of the substance at 300 °C (Buko et al., 2020). The melting points of the active molecules have almost disappeared in the thermograms of the inclusion complexes showing that Q and R located in the inner cavity of the HP-β-CD in amorphous forms (Pralhad and Rajendrakumar 2004; Qu et al., 2021).

3.4.5. *X-Ray diffraction*

As many of the previous studies crystallinity or amorphous state as well as the existence of Q and R in the powdered inclusion complexes were evaluated by XRD analyses (Yan et al., 2019; Liu et al., 2020). XRD diffractograms of Q, R and HP-β-CD showed crystalline structure while T9 and T14 formulations were in amorphous state. T24 showed a little crystallinity most probably exess amount of Q and R (Fig. 5) since it was stated with both ^{1}H-NMR (Fig. 2) and FT-IR (Fig. 3) analyses results (Fig. 5). Crystalline signals of T24 formulation could be attributed to the effect of production method on the structural differences of the final products (Fig. 5).

3.4.6. *In vitro dissolution and release kinetics*

In our study complex formations with HP-β-CD has enhanced the water solubility of Q and R while decreasing the crystallinity of APIs due to the formation of the inclusion complexes. More specifically, as already mentioned, the amount of Q that can be dissolved in water under vigorous agitation for 1 h, has increased from 1.5 µg.mL^{-1} to 945.6 µg.mL^{-1} while for R it was raised to 1901.4 µg.mL^{-1} from 34.3 µg.mL^{-1}, indicating a corresponding increase in the aqueous solubility of both Q and R (Table 2) (Jantarat et al., 2014). Furthermore, *in vitro* release of the APIs from the complexes was much faster than pure Q and R, especially for R, as revealed from the release profiles presented in Fig. 6 (Sri et al., 2007). The *in vitro* release of pure Q reached 22.9 % while it was 26.8 % for R at the end of 2 hours and *in vitro* release of pure R increased up to 64.5 % and 75.8 % with T14 and T24 formulations respectively. However complex formation has decreased the *in vitro* release of Q from 22.9 % to 18.1 % and 15.3 % from T9 and T24 formulations respectively even with enhanced solubility rates. This could

be attributed to much successfull location of Q in the inner cavity of HP-β-CD than R with respect to smaller molecular weight (Liu et al., 2020; Al-Qubaisi et al., 2019). DDSolver computer program was used to determine best fitted kinetic model for our complexes considering the highest rate constant (k) and determination coefficient (r^2) values and the lowest Akaike information criterion (AIC) (Zhang et al., 2010; Güven and Yenilmez 2019; Wójcik-Pastuszka et al., 2019). For pure Q and R best fitted kinetic model was determined as Higuchi while for inclusion complexes Korsmeyer-Peppas model was determined to be the best fitted kinetic model ruled by both diffusion of the drug and dissolution/erosion of the carrier matrix (Table 3) (Al-Heibshy et al.2016).

3.5. Cytotoxicity study

Although CDs are preferred in pharmaceutical formulation to increase the solubility, bioavailability and stability of many drugs, their structure and cytotoxic properties are important factors for more successfull drug delivery (Staedler et al, 2011). Therefore, after the characterization analyses, their cytotoxic properties were evaluated with MTT analyses and, IC_{50} values and cell viability test results were given in Table 4 and Fig. 7. For cytotoxic evaluations NIH-3T3 mouse fibroblast cells were used as non-cancerous cell lines (Danihelova 2013). According to the MTT analyses results pure Q showed cytotoxic effects only with the concentrations over 50 μM, while R and HP-β-CD showed no cytotoxicity with all concentrations on NIH-3T3 cell lines (Table 4, Fig. 7). It has been reported that hydroxypropyl groups reduce the toxic properties of natural α-, β- and γ-CD which also ultimately supports the data of our study (Leroy-Lechat et al., 1994; Laza-Knoerr et al, 2010; Róka et al 2015).

In correlation with the MTT results of pure Q, significiant cell deaths ($p < 0.05$) were observed for T9 complex just after 10 μM while T14 formulation showed no cytotoxicity within the 5-200 μM concentration range on NIH-3T3 cell lines. Incorporation of both flavonoids has slightly influenced the cytotoxicty of T24 compared to T9 and T14 formulations and T24 can be regarded as safe within the range of 5-150 μM on NIH-3T3 cell lines (Table 4, Fig. 7).

Anticancer activity of the prepared formulations were evaluated on two different types of cancer cell lines; MDA-MB-231 and A549 (Li et al., 2021; Komi et al., 2022). Flavonoids showed cell dependant cytotoxicity considering the MTT analyses results (Fig. 7). Both Q and R showed remarkable cell deaths ($p < 0.05$) on MDA-MB-231 cell lines with IC_{50} values at 50 μM and 150 μM respectively while HP-β-CD showed no cytotoxicity at all concentrations (Table 4, Fig. 7). Despite being cytotoxic to NIH-3T3 cell lines, T9 did not show any cytotoxic effect on MDA-MB-231 cell lines. On the contrary T14 formulation showed higher toxicity on MDA-MB-231 than NIH-3T3 cell lines. Presence of both Q and R showed synergistic effect on anticancer activity of the formulation and the lowest cell viability values were detrmined with T24 formulation showing the efficacy of the formulation on MDA-MB-231 cell lines (Fig. 7). For A549 cell lines only pure Q showed cytotoxic effect over 75 μM while R and HP-β-CD were safe within the studied concentration range. T9 and T14 formulations also showed no cytotoxicity while T24 could decrease the viable cell ratios only with 150 μM and higher concentrations (IC_{50}:141.7) (Table 4, Fig. 7). In conclusion MTT analyses results revealed that both pure substances and inclusion complexes showed dose and cell type dependant cytotoxicity which once again highlighted the importance of compositions of formulation and selection of the cells for proper efficacy and evaluation.

3.6. Antioxidant activity

Antioxidant activity of the HP-β-CD inclusion complexes were evaluated by DPPH analyses. In this assay the antioxidant activity of the analyzed sample can easily be determined with the change of the stable deep violet colored radical DPPH to the yellow-colored diphenyl-picrylhydrazine (Alam, Bristi, and Rafiquzzaman 2013) Hadidi et al., 2020; Arya and Raghav 2021). In our study Q has shown the highest antioxidant activity of 93.9 % with 20 $\mu g.mL^{-1}$ while it was 90.3 % with 20 $\mu g.mL^{-1}$ for R (Fig. 8). Among the selected complexes T9 (Q), T14 (R) and T24 (Q/R) the highest activities were 93.8 %, 65.3 % and 93.1 % respectively (Fig. 8). Analyses results revealed that complex formation did not influence the antioxidant activity of Q however it has considerably decreased the antioxydant activity of R (Fig. 7). It has been stated that R showed lower antioxidant capacity than its aglycon, Q, in both DPPH and with other antioxidant activity evaluation methods (López et al., 2003). Incorporation of Q and R together did not enhance the antioxidant activity of the HP-β-CD inclusion complexes in greater extent (Fig. 8) (Cruz-Zúñiga et al., 2016). Former studies also supported these results with the explanation that use of different phenolic compounds as mixtures can decrease the total antioxidant capacity of the stsyem due to the interactions like hydrogen bond formations within the compounds used (Iacopini et al., 2008).

4. Conclusion

In this study Q, R and Q/R inclusion complexes were prepared with HP-β-CD by freeze drying and solvent evaporation methods successfully. ^{1}H-NMR, FT-IR, DSC and XRD analyses were performed for structural determinations. Inclusion complex formation leaded to improved dissolution and water solubility properties of Q and R. According to MTT analysis results, Q and R and inclusion complexes prepared showed dose dependant cytotoxicity even on MDA-MB-231 and A549 cell lines. DPPH analyses results stated that, incorporation of Q into inclusion complexes did not influence the antioxidant activity of the API while the antioxidant activity of R was decreased significantly. Incorporation of Q and R together did not enhance the antioxidant activity of the inclusion complexes in great extent however comparable results were achieved with pure substances. In conclusion, the enhanced *in vitro* dissolution characteristics of Q and R due to formation of HP-β-CD based inclusion complexes, may enable more effective formulations to be developed with potential enhanced bioavailability of the two important flavonoids.

Authors Contributions

Ebru Başaran: Conceptualization, Methodology, Formulation, Validation, Characterization, Experimental Studies, Visualization, Writing- Reviewing and Editing; **A. Alper ÖZTÜRK:** Formulation, Validation, Characterization, Experimental Studies, **Behiye ŞENEL** Investigation of cell culture studies; **Müzeyyen Demirel:** Conceptualization, Methodology, Validation, Visualization, Supervision, Writing-Reviewing and Editing. **Şenay SARICA:** Methodology, Supervision.

Declaration of Competing Interest

The authors declare no conflict of interest.

Acknowledgements

This project was financed by Tokat Special Provincial Administration. Authors would like to acknowledge Eskişehir Technical University, Faculty of Engineering for XRD analyses and Anadolu University Faculty of Pharmacy Doping and Narcotics Analysis Laboratory (DOPNALAB) for FTIR and ^{1}H-NMR analyses.

References

Akyuz, E., Paudel, Y.N., Polat, A.K., Dundar, H.E., Angelopoulou, E., 2021. Enlightening the neuroprotective effect of quercetin in epilepsy: From mechanism to therapeutic opportunities. Epilepsy Behav 115, 107701.

Al-Heibshy, F.N.S., Başaran, E., Demirel, M., 2016. Studies on rosuvastatin calcium incorporated chitosan salt nanoparticles. Lat. Am. J. Pharm. 35, 1065–1076.

Al-Heibshy, F.N.S., Başaran, E., Öztürk, N., Demirel, M., 2020. Preparation and *in vitro* characterization of rosuvastatin calcium incorporated methyl beta cyclodextrin and Captisol® inclusion complexes. Drug. Dev. Ind. Pharm. 46 (9), 1495–1506.
Al-Qubaisi, M.S., Rasedee, A., Flaifel, M.H., et al., 2019. Characterization of thymoquinone/hydroxypropyl-β-cyclodextrin inclusion complex: Application to anti-allergy properties. Eur. J. Pharm. Sci. 133, 167–182.
Alam, N., Bristi, N.J., Rafiquzzaman, Md, 2013. Review on in vivo and in vitro methods evaluation of antioxidant activity. Saudi Pharm. J. 21 (2), 143–152.
Alsaif, N.A., Wani, T.A, Bakheit, A.H, Zargar, S., 2020. Multi-spectroscopic investigation, molecular docking and molecular dynamic simulation of competitive interactions between flavonoids (quercetin and rutin) and sorafenib for binding to human serum albumin. Int J Biol Macromol 15, 2451–2461.
Arya, P., Raghav, Neera, 2021. *In-Vitro* Studies of Curcumin-β-Cyclodextrin Inclusion Complex as Sustained Release System. J. Mol. Struct. 1228 (129774), 1–10.
Buko, V., Zavodnik, I., Palecz, B., et al., 2020. Betulin/2-hydroxypropyl-β-cyclodextrin ınclusion complex: Physicochemical characterization and hepatoprotective activity. J. Mol. Liq. 309 (113118), 1–10.
Celik, S.E., Özyürek, M., Güçlü, K., Apak, R., 2015. Antioxidant Capacity of Quercetin and Its Glycosides in the Presence of β-Cyclodextrins: Influence of Glycosylation on Inclusion Complexation. J. Incl. Phenom. Macro. 83 (3-4), 309–319.
Challa, R., Ahuja, A., Ali, J., Khar, R.K, 2005. Cyclodextrins in drug delivery: An updated review. AAPS PharmSciTech 6 (2), 1–30.
Chen, Y., Fu, R., Xu, J., Du, W., Wang, X., Fang, W., 2017. Thermodynamic (volume and viscosity) of amino acids in aqueous hydroxypropyl-β-cyclodextrin solutions at different temperatures. J. Chem. Thermodyn. 113, 388–393.
Cruz-Zúñiga, J.M., Soto-Valdez, H., Peralta, E., et al., 2016. Development of an Antioxidant Biomaterial by Promoting the Deglycosylation of Rutin to Isoquercetin and Quercetin. Food Chem 204, 420–426.
D'Andrea, G., 2015. Quercetin: A flavonol with multifaceted therapeutic applications? Fitoterapia 106, 256–271.
Danihelová, M., Veverka, M., Šturdík, E., Jantová, S., 2013. Antioxidant action and cytotoxicity on HeLa and NIH-3T3 cells of new quercetin derivatives. Interdiscip Toxicol. 6(4): 209–216.
Ekaette, I., Saldaña, M.D.A., 2021. Ultrasound processing of rutin in food-grade solvents: Derivative compounds, antioxidant activities and optical rotation. Food Chem 15 (344), 1–9, 128629.
Elmi, N., Ghanbarzadeh, G., Ayaseh, A., Sahraee, S., Heshmati, M.K., Hoseini, M., Pezeshki, A., 2021. Physical Properties and Stability of Quercetin Loaded Niosomes: Stabilizing Effects of Phytosterol and Polyethylene Glycol in Orange Juice Model. J. Food. Eng. 296 (110463), 1–11.
FDA 1997. Guidance for Industry: Dissolution Testing of Immediate Release Solid Oral Dosage Forms. 1–17. https://www.fda.gov/media/70936/download.
Franco, P., De Marco, I., 2021. Formation of Rutin–β-Cyclodextrin Inclusion Complexes by Supercritical Antisolvent Precipitation. Polymers 13 (2), 1–15.
Güleç, K., Demirel, M., 2016. Characterization and antioxidant activity of quercetin/methyl-β-cyclodextrin complexes. Curr. Drug. Deliv. 13 (3), 444–451.
Güven, U.M., Yenilmez, E., 2019. Olopatadine hydrochloride loaded kollidon ® SR nanoparticles for ocular delivery: Nanosuspension formulation and *in vitro–in vivo* evaluation. J. Drug. Deliv. Sci. Tec. 51, 506–512.
Hadidi, M., Pouramin, S., Adinepour, F., Haghani, S., Jafari, S.M, 2020. Chitosan nanoparticles loaded with clove essential oil: Characterization, antioxidant and antibacterial activities. Carbohyd. Polym. 236 (116075), 1–8.
Hammoud, Z., Gharib, R., Fourmentin, S., Elaissari, A., Greige-Gerges, H., 2020. Drug-in-hydroxypropyl-β-cyclodextrin-in-lipoid S100/cholesterol liposomes: Effect of the characteristics of essential oil components on their encapsulation and release. Int. J. Pharm. 579 (119151), 1–12.
Iacopini, P., Baldi, M., Storchi, P., Sebastiani, L., 2008. Catechin, Epicatechin, Quercetin, Rutin and Resveratrol in red grape: Content, in vitro antioxidant activity and interactions. J. Food. Compos. Anal. 21 (8), 589–598.
ICH, 1995. European Medicines Agency. Definitions 2, 1–15. November 1994.
ICH Q2 R1, ICH. 2020. 2 Definitions ICH Topic Q 2 (R1) Validation of Analytical Procedures: Text and Methodology.
Ilyich, T.V., Kovalenia, T.A., Lapshina, E.A., Stępniak, A., Palecz, B., Zavodnik, I.B, 2021. Thermodynamic parameters and mitochondrial effects of supramolecular complexes of quercetin with β-cyclodextrins. J. Mol. Liq. 325 (115184), 1–10.
Jantarat, C., Sirathanarun, P., Ratanapongsai, S., Watcharakan, P., Sunyapong, S., Wadu, A., 2014. Curcumin-hydroxypropyl-β-cyclodextrin inclusion complex preparation methods: Effect of common solvent evaporation, freeze drying, and PH shift on solubility and stability of curcumin. Trop. J. Pharm. Res. 13 (8), 1215–1223.
Kamiloglu, S., Sari, G., Ozdal, T., Capanoglu, E., 2020. Guidelines for cell viability assays. Food Frontiers 1, 332–349.
Kellici, T.F., Chatziathanasiadou, M.V., Diamantis, D., Chatzikonstantinou, A.V., Andreadelis, I., Christodoulou, E., Valsami, G., Mavromoustakos, T., Tzakos, A.G., 2016. Mapping the Interactions and Bioactivity of Quercetin (2-Hydroxypropyl)-β-Cyclodextrin Complex. Int. J. Pharm. 511 (1), 303–311.
Komi, D.E.A., Shekari, N., Soofian-kordkandi, P., Javadian, M., Shanehbandi, D., Baradaran, B., Kazemi, T. 2022. Docosahexaenoic acid (DHA) and linoleic acid (LA) modulate the expression of breast cancer involved miRNAs in MDA-MB-231 cell line (article in press). 1-7.
López, M., Martínez, F., Del Valle, C., Ferrit, M., Luque, R., 2003. Study of phenolic compounds as natural antioxidants by a fluorescence method. Talanta 60 (2-3), 609–616.
Laquintana, V., Asim, M.H., Lopedota, A., Cutrignelli, A., Lopalco, A., Franco, M., Bernkop-Schnürch, A., Denora, N., 2019. Thiolated hydroxypropyl-β-cyclodextrin as mucoadhesive excipient for oral delivery of budesonide in liquid paediatric formulation. Int. J. Pharm. 572 (118820), 1–12.
Laza-Knoerr, A.L., Gref, R., Couvreur, P., 2010. Cyclodextrins for drug delivery. J. Drug. Target. 18 (9), 645–656.
Leroy-Lechat, F., Wouessidjewe, D., Andreux, J.P., Puisieux, F., Duchene, D., 1994. Evaluation of the cytotoxicity of cyclodextrins and hydroxypropylated derivatives. Int. J. Pharm. 101, 97–103.
Li, N., Chen, C., Zhu, H., Shi, Z., Sun, J., Chen, L., 2021. Discovery of novel celastrol-triazole derivatives with Hsp90-Cdc37 disruption to induce tumor cell apoptosis. Bioorg. Chem. 111 (104867), 1–10.
Liu, C.H., Guan, W.L., Wei, C.W., Chun, C.W., 2020. Encapsulating curcumin in ethylene diamine-β-cyclodextrin nanoparticle improves topical cornea delivery. Colloid. Surface. B 186, 1–9.
Liu, J., Ding, X., Fu, Y., Xiang, C., Yuan, Y., Zhang, Y., Yu, P., 2021. Cyclodextrins based delivery systems for macro biomolecules. Eur. J. Med. Chem. 212, 1–23.
Loftsson, T., Dagný, H., Már, M., 2005. Evaluation of cyclodextrin solubilization of drugs. Int. J. Pharm. 302 (1–2), 18–28.
Manta, K., Papakyriakopoulou, P., Chountoulesi, M., Diamantis, D.A., Spaneas, D., Vakali, V., Naziris, N., et al., 2020. Preparation and Biophysical Characterization of Quercetin Inclusion Complexes with β-Cyclodextrin Derivatives to Be Formulated as Possible Nose-to-Brain Quercetin Delivery Systems. Mol. Pharm. 17 (11), 4241–4255.
Melo, C.O., Rodrigues, M.S.S., da Silva, M.V.S., Marcelino, H.R., Rabello, M.M., de Moura, R.O., Oliveira, E.E., 2020. Preparation and characterization of spiro-acridine derivative and 2-hydroxypropyl-β-cyclodextrin ınclusion complex. J. Mol. Struct. 1222 (128945), 1–10.
Mosmann, T., 1983. Rapid colorimetric assay for cellular growth and survival: application to proliferation and cytotoxicity assays. J. Immunol. Methods. 16 65 (1-2), 55–63.
Nicolescu, C., Arama, C., Monciu, C.M., 2010. Preparation and characterization of inclusion complexes between repaglinide and β-cyclodextrin, 2-hydroxypropyl-β-cyclodextrin and randomly methylated β-cyclodextrin. Farmacia. 58(1), 78–88.
Nicoletti, C.D., de Sá Haddad Queiroz, M., Guimarães de Souza Lima, C., de Carvalho da Silva, F., Futuro, D.O., Ferreira, V.F., 2020. An improved method for the preparation of β-lapachone:2-hydroxypropyl-β-cyclodextrin inclusion complexes. J. Drug. Deliv. Sci. Tec. 58 (101777), 1–8.
Paczkowska, M., Mizera, M., Piotrowska, H., Szymanowska-Powałowska, D., Lewandowska, K., Goscianska, J., Pietrzak, R., et al., 2015. Complex of Rutin with β-Cyclodextrin as Potential Delivery System. PLoS ONE 10 (3), 1–16.
Park, K.H., Choi, J.M., Cho, E., Jeong, D., Shinde, V.V., Kim, H., Choi, Y., Jung, S., 2017. Enhancement of Solubility and Bioavailability of Quercetin by Inclusion Complexation with the Cavity of Mono-6-deoxy-6-aminoethylamino-β-cyclodextrin. B. Kor. Chem. Soc. 38, 880–889.
Patil, A.G., Jobanputra, A.H., 2015. Rutin-chitosan nanoparticles: Fabrication, characterization and application in dental disorders. Polym-Plast. Technol. 54 (2), 202–208.
Paudel, K.R., Wadhwa, R., Tew, X.N., Lau, N.J.X., Madheswaran, T., Panneerselvam, J., Zeeshan, F., Kumar, P., Gupta, G., Anand, K., Singh, S.K., Jha, N.K., MacLoughlin, R., Hansbro, N.G., Liu, G., Shukla, S.D., Mehta, M., Hansbro, P.M., Chellappan, D.K., Dua, K., 2021. Rutin loaded liquid crystalline nanoparticles ınhibit non-small cell lung cancer proliferation and migration in vitro. Life Sci. 1 276 (119436), 1–11.
Pereira, A.B., Silva, A.M., Barroca, M.J., Marques, M.P.M., Braga, S.S, 2020. Physicochemical Properties, Antioxidant Action and Practical Application in Fresh Cheese of the Solid Inclusion Compound γ-Cyclodextrin•quercetin, in Comparison with β-Cyclodextrin•quercetin. Arab. J. Chem. 13 (1), 205–215.
Pinheiro, R.G.R., Granja, A., Loureiro, J.A., Pereira, M.C., Pinheiro, M., Neves, A.R., Reis, S., 2020. Quercetin Lipid nanoparticles functionalized with transferrin for Alzheimer's disease. Eur. J. Pharm. Sci. 148 (105314), 1–11.
Pralhad, T., Rajendrakumar, K., 2004. Study of freeze-dried quercetin-cyclodextrin binary systems by DSC, FT-IR, X-Ray siffraction and SEM analysis. J. Pharmaceut. Biomed. 34 (2), 333–339.
Qu, Y., Sun, X., Ma, L., Li, C., Xu, Z., Ma, W., Zhou, Y., Zhao, Z., Ma, D., 2021. Therapeutic effect of disulfiram ınclusion complex embedded in hydroxypropyl-β-cyclodextrin on ıntracranial glioma-bearing male rats via ıntranasal route. Eur. J. Pharm. Sci. 156 (105590), 1–7.
Róka, E., Ujhelyi, Z., Deli, M., Bocsik, A., Fenyvesi, É., Szente, L., Fenyvesi, F., Vecsernyés, M., Váradi, J., Fehér, P., Gesztelyi, R., Félix, C., Perret, F., Bácskay, I.K., 2015. Evaluation of the cytotoxicity of α-cyclodextrin derivatives on the Caco-2 cell line and human erythrocytes. Molecules. 11 20 (11), 20269–20285.
Rahman, F., Tabrez, S., Ali, R., Alqahtani, A.S., Ahmed, M.Z., Rub, A., 2021. Molecular docking analysis of rutin reveals possible ınhibition of SARS-CoV-2 vital proteins. J. Tradit. Complem. Med. 96 (3), 450–469.
Rebolledo, V., Otero, M.C., Delgado, J.M., Torres, F., Herrera, M., Ríos, M., Cabañas, M., Martinez, J.L., Rodríguez-Díaz, M., 2021. Phytochemical profile and antioxidant activity of extracts of the peruvian peppertree *Schinus areira* L. from Chile. Saudi. J. Biol. Sci. 28 (1), 1052–1062.
Remanan, M.K., Zhu, F., 2021. Encapsulation of rutin using quinoa and maize starch nanoparticles. Food Chem 353 (128534), 1–14.
Sahinturk, V., Kacar, S., Vejselova, D., Kutlu, H.M, 2018. Acrylamide exerts ıts cytotoxicity in NIH/3T3 fibroblast cells by apoptosis. Toxicol. Ind. Health. 34 (7), 481–489.
Savic, I.M., Savic-Gajic, I.M., Nikolic, V.D., Nikolic, L.B., Radovanovic, B.C., Milenkovic-Andjelkovic, A., 2016. Enhencemnet of Solubility and Photostability of Rutin by Complexation with β-Cyclodextrin and (2-Hydroxypropyl)-β-Cyclodextrin. J. Incl. Phenom. Macro. 86 (1–2), 33–43.
Shen, J., Burgess, D.J, 2013. In vitro dissolution testing strategies for nanoparticulate drug delivery systems: recent developments and challenges. Drug. Deliv. Transl. Re. 3 (5), 409–415.

Sri, K.V., Kondaiah, A., Ratna, J.V., Annapurna, A., 2007. Preparation and characterization of quercetin and rutin cyclodextrin ınclusion complexes. Drug. Dev. Ind. Pharm. 33 (3), 245–253.

Staedler, D., Idrizi, E., Kenzaoui, B.H., Juillerat-Jeanneret, L., 2011. Drug combinations with quercetin: doxorubicin plus quercetin in human breast cancer cells. Cancer. Chemother. Pharmacol. 68 (5), 1161–1172.

Tripathi, D., Gupta, P.K., Banerjee, S., Kulkarni, S., 2021. Quercetin induces proteolysis of mesenchymal marker vimentin through activation of caspase-3, and decreases cancer stem cell population in human papillary thyroid cancer cell line. Phytomedicine Plus 1 (100108), 1–9.

Valencia, M.S., Franco da Silva Júnior, M., Xavier Júnior, F.H., de Oliveira Veras, B., Fernanda de Oliveira Borba, E., Gonçalves da Silva, T., Xavier, V.L., Pessoa de Souza, M., Carneiro-da-Cunha, M.G., 2021. Bioactivity and cytotoxicity of quercetin-loaded, lecithin-chitosan nanoparticles. Biocatal. Agric. Biotechnol. 31 (101879), 1–10.

Wójcik-Pastuszka, D, Krzak, J, Macikowski, B., Berkowski, R., Osiński, B., Musiał, W., 2019. Evaluation of the Release Kinetics of a Pharmacologically Active Substance from Model Intra-Articular Implants Replacing the Cruciate Ligaments of the Knee. Materials 12 (1202), 1–13.

Wang, T., Guo, N., Wang, S.X., Kou, P., Zhao, C.J., Fu, Y.J., 2018. Ultrasound-negative pressure cavitation extraction of phenolic compounds from blueberry leaves and evaluation of its DPPH radical scavenging activity. Food. Bioprod. Process. 108, 69–80.

Wang, H., Luo, J., Zhang, Y., He, D., Jiang, R., Xie, X., Yang, Q., Li, K., Xie, J., Zhang, J., 2020. Phospholipid/hydroxypropyl-β-cyclodextrin supramolecular complexes are promising candidates for efficient oral delivery of curcuminoids. Int. J. Pharm. 582 (119301), 1–16.

Wang, X.Q., Wang, W., Peng, M., Zhang, X.Z, 2021. Free Radicals for Cancer Theranostics. Biomaterials 266 (120474), 1–15.

Yan, C., Liang, N., Li, Q., Yan, P., Sun, S., 2019. Biotin and arginine modified hydroxypropyl-β-cyclodextrin nanoparticles as novel drug delivery systems for paclitaxel. Carbohyd. Polym. 216, 129–139.

Zhang, Y., Huo, M., Zhou, J., Zou, A., Li, W., Yao, C., Xie, S., 2010. DDSolver: An add-in program for modeling and comparison of drug dissolution profiles. AAPS Journal 12 (3), 263–271.

Zhang, J., Ning, L., Wang, J., 2020. Dietary Quercetin attenuates depressive-like behaviors by ınhibiting astrocyte reactivation in response to stress. Biochem. Bioph. Res. Co. 533 (4), 1338–1346.

Zhao, Z., Dong, L., Wu, Y., Lin, F., 2011. Preliminary separation and purification of rutin and quercetin from Euonymus Alatus (Thunb.) siebold extracts by macroporous resins. Food. Bioprod. Process. 89 (4), 266–272.

Zheng, Ying, Chow, Albert H.L., 2009. Production and Characterization of a Spray-Dried Hydroxypropyl-β- Cyclodextrinquercetin Complex Spray-Dried Hydroxypropyl-β-Cyclodextrin/Quercetin Complex. Drug Dev. Ind. Pharm. 35 (6), 727–734.

Zhou, Y., Niu, B., Luo, Q., Zhang, Y., Quan, G., Pan, X., Wu, C., 2020. Cyclodextrin-Based Metal-Organic Frameworks for Pulmonary Delivery of Curcumin with Improved Solubility and Fine Aerodynamic Performance. Int. J. Pharm. 588 (119777), 1–8.